Dual mechanical behaviour of hydrogen in stressed silicon nitride thin films

F. Volpi, M. Braccini, Arnaud Devos, G. Raymond, A. Pasturel, Pascal Morin

Journal of Applied Physics

Dual mechanical behaviour of hydrogen in stressed silicon nitride thin films

Cite as: J. Appl. Phys. **116**, 043506 (2014); https://doi.org/10.1063/1.4887814
Submitted: 23 April 2014 • Accepted: 26 June 2014 • Published Online: 24 July 2014

F. Volpi, M. Braccini, A. Devos, et al.

Dual mechanical behaviour of hydrogen in stressed silicon nitride thin films

F. Volpi,[1,2,a)] M. Braccini,[1,2] A. Devos,[3] G. Raymond,[1,2,4] A. Pasturel,[1,2] and P. Morin[4]
[1]*Univ. Grenoble Alpes, SIMAP, F-38000 Grenoble, France*
[2]*CNRS, SIMAP, F-38000 Grenoble, France*
[3]*IEMN, UMR 8520 CNRS, Avenue Poincarré - CS 60069 - 59652 Villeneuve d'Ascq Cedex, France*
[4]*STMicroelectronics, 850 rue Jean Monnet, 38926 Crolles Cedex, France*

(Received 23 April 2014; accepted 26 June 2014; published online 24 July 2014)

In the present article, we report a study on the mechanical behaviour displayed by hydrogen atoms and pores in silicon nitride (SiN) films. A simple three-phase model is proposed to relate the physical properties (stiffness, film stress, mass density, etc.) of hydrogenated nanoporous SiN thin films to the volume fractions of hydrogen and pores. This model is then applied to experimental data extracted from films deposited by plasma enhanced chemical vapour deposition, where hydrogen content, stress, and mass densities range widely from 11% to 30%, −2.8 to 1.5 GPa, and 2.0 to 2.8 g/cm^3, respectively. Starting from the conventional plotting of film's Young's modulus against film porosity, we first propose to correct the conventional calculation of porosity volume fraction with the hydrogen content, thus taking into account both hydrogen mass and concentration. The weight of this hydrogen-correction is found to evolve linearly with hydrogen concentration in tensile films (in accordance with a simple "mass correction" of the film density calculation), but a clear discontinuity is observed toward compressive stresses. Then, the effective volume occupied by hydrogen atoms is calculated taking account of the bond type (N-H or Si-H bonds), thus allowing a precise extraction of the hydrogen volume fraction. These calculations applied to tensile films show that both volume fractions of hydrogen and porosity are similar in magnitude and randomly distributed against Young's modulus. However, the expected linear dependence of the Young's modulus is clearly observed when both volume fractions are added. Finally, we show that the stiffer behaviour of compressive films cannot be only explained on the basis of this (hydrogen + porosity) volume fraction. Indeed this stiffness difference relies on a dual mechanical behaviour displayed by hydrogen atoms against the film stress state: while they participate to the stiffness in compressive films, hydrogen atoms mainly behave like pores in tensile films where they do not participate to the film stiffness. © *2014 AIP Publishing LLC*.
[http://dx.doi.org/10.1063/1.4887814]

I. INTRODUCTION

Silicon nitride (SiN) thin films are widely used for both their functional properties (electrical insulation, optical refraction, low permeation to impurities, etc.) and for their mechanical properties (stiffness, hardness, stress driver, etc.).[1,2] In particular, SiN has been widely used in microtechnology process flow for diverse applications:[3,4] as Etch Stop Layers (ESLs) for their hardness and chemical resistance,[3] as encapsulating layers for their ability to prevent copper diffusion in metal interconnections,[5] as passivation layers for their ability to prevent moisture absorption,[3] as capping passivating layers in microsystems,[6] as anti-reflective coatings for solar cells,[7] and as stress drivers to improve electron mobility of n-MOS transistors.[8]

All these SiN thin films are usually amorphous (or nanocrystalline) and hydrogenated. Their chemical organisation has been extensively studied numerically.[9–12] The disordered structure comes from the low deposition temperature required for device fabrication (usually ranging within 200–500 °C) and leads to cavities at the nanometer-scale. Hydrogen atoms are inevitably introduced during film processing, usually based on CVD process (for Chemical Vapor Deposition): LPCVD (Low Pressure CVD, PECVD (Plasma Enhanced CVD), etc. Hydrogen atoms are known to improve the SiN insulating properties (by saturating broken bonds).[9] The physical chemistry of hydrogen incorporation in PECVD-grown SiN films has been widely reported,[13–15] as well as the enhancement of compressive stress build-up through atomic peening mechanism.[16,17]

Numerous works have been reported on the empirical relationship between hydrogen content and SiN structural properties (density, mechanical stress, stiffness, hardness, etc.).[18–21] In particular, the mechanism of stress build-up against the chemical reactions taking place during film processing (or post-process treatments) is well-documented.[21,22] However, hydrogen and porosity volume fractions are rarely discriminated, thus preventing the identification of the prevailing phenomenon. In addition, to our knowledge, no data are available on a dual mechanical behaviour displayed by hydrogen in tensile and compressive SiN films. Our results will be confronted to works reported on other iono-covalent amorphous ceramics: carbon, silicon, and germanium amorphous films.

a)Author to whom correspondence should be addressed. Electronic mail: fabien.volpi@simap.grenoble-inp.fr.

II. EXPERIMENTAL TECHNIQUES

A. Film processing

The silicon nitride films were deposited by PECVD over silicon substrates at 400 °C. Tensile films were deposited with a multilayer approach: the deposition process alternated short deposition steps (few nm-thick) with pure nitrogen plasma treatments (for few seconds). The films were then formed by sequential deposition/plasma treatment steps. A more detailed description of the deposition process of these tensile films can be found in Morin *et al.*[8] Compressive films were monolayer films deposited at low pressure (2 Torr) and increased plasma power (75 W) to improve atomic peening. The deposited thicknesses of both film families range from 130 to 680 nm.

B. Physical and chemical characterizations

The films were characterized with standard clean-room dedicated tools. Chemical bond types and densities were measured by combining spectroscopic ellipsometry (FX100 ellipsometer from KLA Tencor) and Fourier Transform InfraRed (FTIR) spectroscopy (BIO RAD QS 2200A from Accent). A specific analysis was applied to obtain an overall description of the film chemistry,[8] thus providing quantitative bond concentration results of 10^{17} bonds cm^{-2} with an uncertainty of ± 0.5. Film density was measured, thanks to a high-precision weighting machine (Mentor SP3 from Metryx). The mechanical stress was evaluated by wafer curvature measurement from Stoney's formula (accuracy better than 10 MPa for a 350 nm thick film). The film elastic stiffness (Young's modulus) has been measured by picosecond ultrasonic technique, which is based on acoustic wave propagation. A more detailed description of the technique is given in Refs. 23–25 and details of the measurement on our samples are reported in Ref. 26. In our case, the precision on the measured stiffness is 2%.

III. MODELLING OF HYDROGEN-DOPED NANOPOROUS SiN FILMS: SIMPLE THREE-PHASE MODEL

A. Phase definition

The structure of hydrogen-doped nanoporous SiN films is rather complex at the atomic scale and requires *ab initio* calculations for proper modelling.[12] The long-range disorder of this amorphous material is concomitant to nanoscale porosity and of hydrogen atoms (that saturate dangling bonds). Even though the characteristic lengths of these features reach the scale of electron clouds, we propose to model this system through meso-scale continuous media with sharp interfaces. Within this frame, we propose to describe the film as the coexistence of three distinct phases (Figure 1):

- Phase 1: Dense SiN (hydrogen and pore-free)—This phase, which constitutes the main skeleton of the film, is made up of Si-N and Si-Si bonds. Proportions of these bonds depend on the film stoichiometry. N-N bonds are known for being absent of such films.[12] The film stiffness is supposed to be mainly driven by this phase.

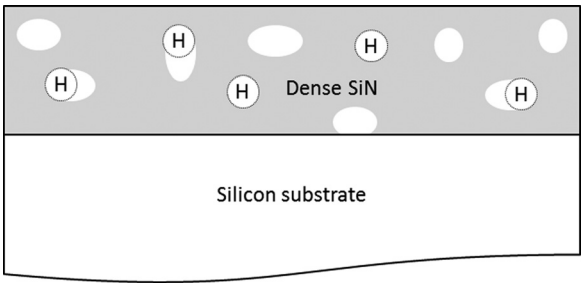

FIG. 1. Three-phase model of hydrogen-doped nanoporous SiN film. The main grey area represents the "Dense SiN" phase. White areas represent pores. H-marked areas represent hydrogen atoms.

- Phase 2: Hydrogen atoms—These atoms are either bonded to silicon or nitrogen atoms. In terms of chemical bonding, the remarkable specificity of hydrogen atoms is that they only bind once, meaning that hydrogen atoms terminate atom chains. As a consequence, they should not transmit mechanical stress from one atom to another, suggesting that hydrogen should not participate to the global film stiffness.
- Pores—Individual nanoscale cavities are usually found in amorphous thin films. They are due to the long-range disorder of atom chains and to the induced bond angle misfit. In terms of mechanical stiffness, they constitute a zero-stiffness phase.

For further clarity, the sum of both hydrogen and pore phases will be called the "negative phase," as opposed to the "Dense SiN" phase that constitutes the "positive phase" of the film.

B. Equation statement

From the above system definition, one can define different magnitudes describing volume and mass-related properties:

V_{Phase}, m_{Phase}, d_{Phase}, and f_{Phase}: the volume (in cm^3), mass (in g), mass density (in g/cm^3), and volume fraction of the indexed phase, respectively.

f_{Phase} is defined as

$$f_{Phase} = \frac{V_{Phase}}{V_{Film}}. \tag{1}$$

The indexed phase can be either of the followings: Film (i.e., the entire film, including the three phases), Dense SiN, H (for Hydrogen), Pore, and H + Pore (i.e., the "negative phase").

From these magnitudes, the following equations can be stated:

(a) Volume relation

$$V_{Film} = V_{Dense\ SiN} + V_H + V_{Pore}. \tag{2}$$

(b) Mass relations

$$m_{Film} = m_{Dense\ SiN} + m_H + m_{Pore}, \tag{3a}$$

$$m_{Pore} = 0, \tag{3b}$$

$$m_H = [H] \times V_{Film} \times (P_H \times u). \tag{3c}$$

With $[H]$ the hydrogen concentration (in cm^{-3}) in the film and $(P_H \times u)$ the atomic mass of hydrogen, $P_H = 1.008$ and $u = 1.66 \times 10^{-24}$ g.

(c) Mass density relations

$$d_{Film} = \frac{m_{Film}}{V_{Film}}, \tag{4a}$$

$$d_{Dense\ SiN} = \frac{m_{Dense\ SiN}}{V_{Dense\ SiN}}. \tag{4b}$$

With $d_{Dense\ SiN} = 3.2\,\mathrm{g/cm^3}$.

(d) Volume fraction relations

$$f_{Dense\ SiN} = \frac{V_{Dense\ SiN}}{V_{Film}}, \tag{5a}$$

$$f_H = \frac{V_H}{V_{Film}}, \tag{5b}$$

$$f_{Pore} = \frac{V_{Pore}}{V_{Film}}, \tag{5c}$$

$$f_{H+Pore} = \frac{V_H + V_{Pore}}{V_{Film}}. \tag{5d}$$

The combination of Eqs. (2), (3a), (3c), (4a), (4b), and (5d) leads to

$$f_{H+Pore} = f_H + f_{Pore}, \tag{6a}$$

$$f_{H+Pore} = 1 - \frac{d_{Film}}{d_{Dense\ SiN}} + \frac{[H] \times (P_H \times u)}{d_{Dense\ SiN}}. \tag{6b}$$

C. Hydrogen modelling

At this stage, a more detailed description of the volume occupied by hydrogen atoms is required. Within the frame of the present meso-scale model, we propose to apply a hard-sphere model to the hydrogen atom. The quantitative criterion further used to describe the volume occupied by hydrogen is the hydrogen radius R_H. R_H can be defined as the smallest distance beyond which a neighbouring atom does not bind chemically with hydrogen (no hybridization). For free hydrogen atoms, R_H is the Van der Waals radius (120 pm, from Ref. 27). However, in the case of bonded hydrogen, R_H should be handled with care. In SiN films, hydrogen either binds to silicon or to nitrogen. Because of the s-character of the hydrogen orbital, the electronic probability density remains spherical and centered on the hydrogen nucleus; thus, the smallest distance before chemical bonding is given by the atomic bond length (Figure 2). From this description, the hydrogen volume fraction can now be expressed directly

$$f_H = \left(\frac{4\pi}{3} R_H^3\right) \times [H]. \tag{7}$$

Finally, combining Eqs. (6a), (6b), and (7) leads to

$$f_{Pore} = 1 - \frac{d_{Film}}{d_{Dense\ SiN}} + \frac{[H] \times (P_H \times u)}{d_{Dense\ SiN}} - \left(\frac{4\pi}{3} R_H^3\right) \times [H]. \tag{8}$$

In addition, because of the electronegativity difference between the involved atoms ($\chi_{Si} = 1.9\,\mathrm{eV}$, $\chi_H = 2.2\,\mathrm{eV}$, and $\chi_N = 3.04\,\mathrm{eV}$), one can expect slightly different electron shell extensions and bond lengths for Si-H and N-H bonds. In accordance with this trend, numerical simulations have shown that $d_{N\text{-}H} = 115\,\mathrm{pm}$ and $d_{Si\text{-}H} = 150\,\mathrm{pm}$ (from Ref. 11), in close accordance with Refs. 28, 10, and 12.

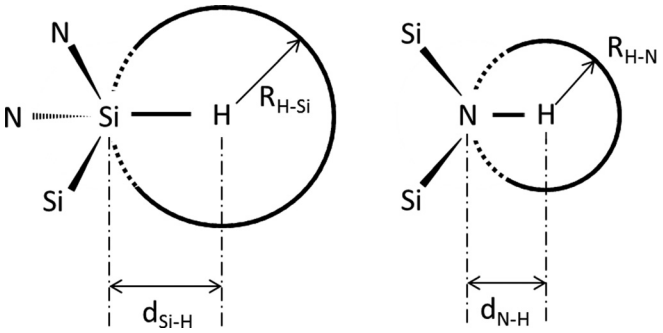

FIG. 2. Hard-sphere schematics of the hydrogen radius R_H for both Si-H (left) and N-H (right) bonds.

IV. POROSITY-DEPENDENCE OF STIFFNESS: HYDROGEN-CORRECTION

In literature, the stiffness of porous materials (and of SiN films in particular) is either represented against material density[29–31] or against porosity volume fraction.[32,33] Both representations are equivalent as long as porosity is the only phase constituting the "negative phase" of the dense SiN phase (i.e., in almost hydrogen-free films). Indeed in that case, the volume fraction of pores is easily found

$$f'_{Pore} = 1 - \frac{d_{Film}}{d_{Dense\ SiN}}. \tag{9}$$

With f'_{Pore} the pore volume in hydrogen-free SiN films, and $d_{Dense\ SiN} = 3.2\,\mathrm{g/cm^3}$.

Within the frame of our three-phase model, the corresponding magnitude is now f_{H+Pore} (which is the negative phase of the dense SiN phase). This f_{H+Pore} magnitude simply corrects the effective mass of the material that responds mechanically: as stated above, hydrogen atoms should not respond mechanically, while the mass of these atoms is taken into account in the measured film mass. The analytical expression of this hydrogen-correction (X_H) is the last term of Eq. (6b)

$$X_H = \frac{[H] \times (P_H \times u)}{d_{Dense\ SiN}}. \tag{10a}$$

This leads to

$$f_{H+Pore} = f'_{Pore} + X_H. \tag{10b}$$

For hydrogen-free films, this hydrogen-correction X_H is nil and f_{H+Pore} equals f_{Pore}. In hydrogenated films, the stiffness can now be represented against the hydrogen-corrected porosity (i.e., against f_{H+Pore}) (Figure 3).

Both the stiffness range (90–150 GPa and 165–230 GPa for tensile and compressive films, respectively) and the density range (2.0–2.5 g/cm^3 and 2.5–2.8 g/cm^3 for tensile and compressive films, respectively) are consistent with data

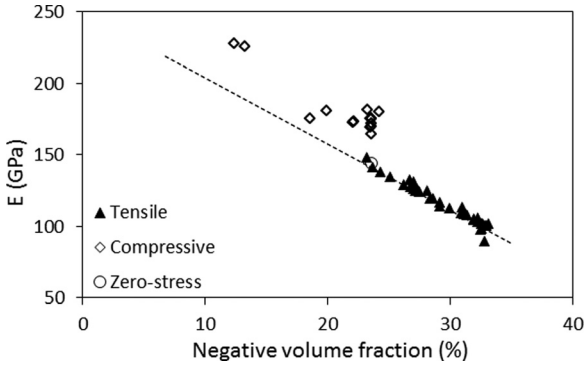

FIG. 3. Young's modulus of tensile and compressive films against the negative phase volume fraction (f_{H+Pore}).

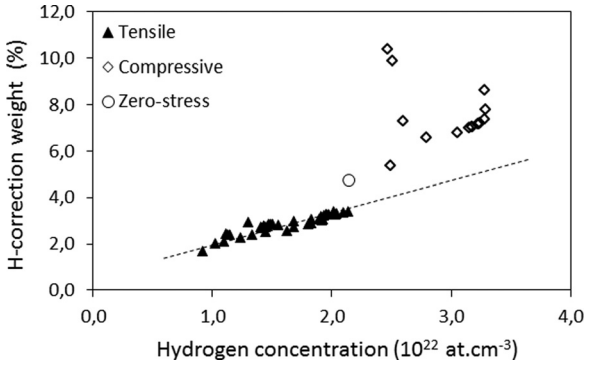

FIG. 4. Weight of the hydrogen-correction X_H (in percentage of the negative phase volume fraction) against the hydrogen concentration.

found in literature on PECVD-grown SiNH films.[31,34] The trend found in Figure 3 is also consistent with the stiffness decrease with porosity increase[29] or with the average coordination number reduction[35] described in literature. It can be seen that tensile and compressive samples draw two distinct data clouds. Both clouds display a linear dependence of stiffness against the hydrogen-corrected porosity (clear linear dependence for tensile films, more dispersed for compressive films because of the lower number of points). This is in agreement with literature on hydrogen-doped SiN films.[20] Extrapolation of the "tensile-films" trend (dotted line) shows that for similar f_{H+Pore}, compressive films are stiffer than tensile films.

The weight of the hydrogen-correction X_H has been calculated numerically for both populations. This weight (given in percentage of the negative phase fraction (f_{H+Pore}) is reported in Table I.

This calculation first shows that this hydrogen-correction X_H is more relevant in compressive films (~9.0%) than in tensile films (~3.3%): while this correction may fit within the error bars in tensile films, it definitely has to be taken into account in compressive films. Table I also shows that the average hydrogen content is larger in compressive films. In order to check if the different weight observed on both populations is related to the hydrogen concentration or to the mechanical behaviour of hydrogen, the weight of this hydrogen-correction is represented in Figure 4 against hydrogen concentration.

A nearly linear dependence of the hydrogen-correction weight with hydrogen concentration is found for tensile films. The slope (which is proportional to the reciprocal of f_{H+Pore}) only slightly varies with hydrogen content. This linearity matches with the expected mechanical behaviour of hydrogen: as hydrogen atoms only terminate SiN matrix bonds they cannot transmit mechanical stress, thus they behave as a zero-stiffness phase (i.e., as ideal pores). Within this frame, the hydrogen-correction X_H simply subtracts the hydrogen mass from the measured film mass and does not affect the film stiffness. As it may be seen in Figure 4, its weight simply evolves linearly with hydrogen concentration in tensile films.

The extrapolation of the "tensile-films" trend to the "compressive-films" (dotted line) range clearly shows that the intrinsic behaviour of hydrogen differs drastically for both populations. This gap strongly suggests that hydrogen atoms do not behave like ideal pores in compressive films. This dual behaviour description will be supported below.

TABLE I. Hydrogen-related data in tensile and compressive films.

	Average weight of the hydrogen-correction (X_H/f_{H+Pore})	Average hydrogen concentration ($10^{22}/cm^3$)
Tensile films	3.3% +/−0.7%	1.6% +/−0.4%
Compressive films	9.0% +/−2%	3.0% +/−0.3%

V. ESTIMATION OF THE VOLUME OCCUPIED BY HYDROGEN ATOMS

In order to study the pore-like behaviour of hydrogen in tensile films, we propose to estimate the effective volume they occupy in the film. Equation (8) reports the dependence of pore volume fraction (f_{Pore}) against hydrogen radius (R_H). As these two magnitudes are not available experimentally independently, we first propose to assume that porosity is nil on all the samples (this "zero-porosity" assumption will be discussed and corrected afterwards). Under this assumption, R_H can be extracted from Eq. (8) with $f_{Pore} = 0$ (leading to Eq. (11)) and then plotted against film stress (Figure 5)

$$R_H = \sqrt[3]{\frac{3}{4\pi[H]}\left[1 - \frac{d_{Film} - [H] \times (P_H \times u)}{d_{Dense\ SiN}}\right]}. \qquad (11)$$

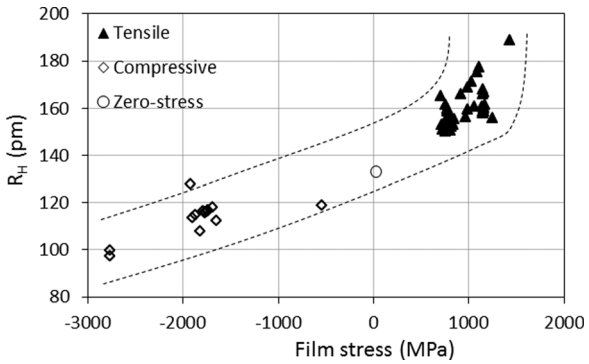

FIG. 5. Calculated hydrogen radius R_H against film stress. Dashed lines are guides for the eye.

This plot confirms the different behaviours of hydrogen within both populations: while the "tensile" R_H cloud spans from 143 to 189 pm, the "compressive" R_H cloud spans from 100 to 128 pm. The two dotted lines are given to guide the eye from the "tensile" to "compressive" clouds. It appears that a transition occurs around 120–140 pm for zero-stress condition.

The calculation of R_H under this "zero-porosity" assumption considers that the negative phase (i.e., hydrogen atoms + pores) is fully occupied by hydrogen atoms. However, nanoscale porosity is thermodynamically stable in tensile films and is always found in such films, thus this "zero-porosity" assumption leads to an overestimation of R_H for tensile films: the calculated R_H hides pores within the hydrogen volume fraction. The case of compressive films will be discussed afterwards.

Despite the simplicity of our model, the R_H transition range at zero-stress (120–140 pm) is in very good agreement with numerical modelling[11] that state that $d_{N\text{-}H} = 115$ pm and $d_{Si\text{-}H} = 150$ pm. However, as this nearest neighbour distance varies so greatly (~50% from N-H to Si-H bonding), one can expect that the concentration of N-H and Si-H bonds should affect the calculated effective R_H (till this point our calculations do not discriminate N-H from Si-H bonds). Figure 6 represents the ratio of Si-H bond concentration over the total concentration of hydrogen bonds (Si-H + N-H) in our films. This plot clearly shows that the Si-H bonds are almost absent from compressive films (Si-H concentration varies from undetectable to ~5%). This result is explained by the steric effect associated to the large dimension of Si-H that prevents these bonds to form during the processing of compressive films. On the contrary, tensile films display much larger Si-H bond concentration (25% in average, up to 65%) confirming that the steric effect is much less important in tensile films.

This discrepancy between tensile and compressive films allows a better understanding of Figure 5: the large R_H calculated in tensile films actually corresponds to the coexistence of hydrogen atoms occupying large volumes (when bonded to Si) and hydrogen atoms occupying smaller volumes (when bonded to N), while the small R_H calculated in compressive films corresponds to the smaller volumes occupied by the N-H bonds.

From these observations, it is now possible to calculate directly the f_H with an appropriate choice of R_H: 115 pm or 150 pm for hydrogen atoms bonded to nitrogen or to silicon, respectively. Equation (7) can then be improved by weighting the hydrogen bond concentration by the corresponding R_H. The hydrogen volume fraction can then be expressed as

$$f_H = \left(\frac{4\pi}{3}R_{H-Si}^3\right) \times [\mathrm{Si}-H] + \left(\frac{4\pi}{3}R_{H-N}^3\right) \times [N-H]. \tag{12}$$

With $[\mathrm{Si}-H]$ and $[N-H]$ the concentrations of Si-H and N-H bonds, respectively. $R_{H\text{-}Si} = 150$ pm and $R_{H\text{-}N} = 115$ pm. This exact expression of the hydrogen volume fraction now replaces Eq. (7) for further calculations.

As Eq. (6a) remains valid, its combination with Eq. (12) allows the discrimination of volume fractions of both hydrogen and pores. Thus, the evolution of tensile film stiffness against the two volume fractions f_H and f_{Pore} can be plotted (Figures 7 and 8). One can see that no linear dependence is observed either for hydrogen or pore volume fractions. Only their sum (f_{H+Pore}, also shown) leads to a linear dependence with Young's modulus (i.e., the linear dependence already shown in Figure 3). As f_H and f_{Pore} are of the same order of magnitude, none of them forces this linearity. This confirms our previous suggestion on the mechanical behaviour of hydrogen within tensile films: hydrogen atoms behave like a "zero-stiffness" phase (i.e., like pores), inducing a linear

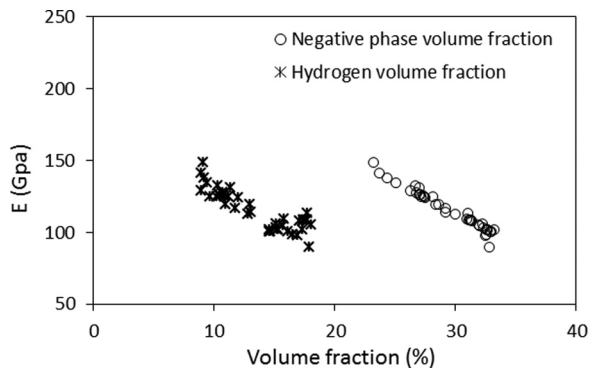

FIG. 7. Young's modulus of tensile films against the volume fractions of hydrogen (f_H) and of the negative phase (f_{H+Pore}).

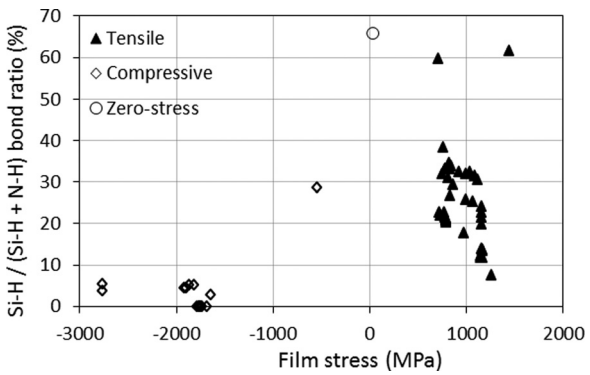

FIG. 6. Ratio of Si-H bonds over the total concentration of hydrogen bonds (Si-H + N-H) against the film stress.

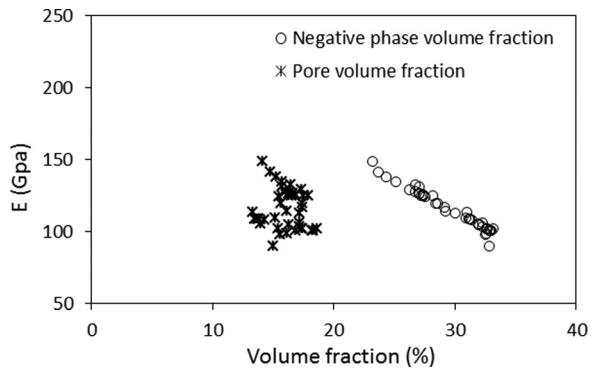

FIG. 8. Young's modulus of tensile films against the volume fractions of pores (f_{Pore}) and of the negative phase (f_{H+Pore}).

dependence of the film stiffness with the fraction of these two "zero-stiffness" phases.

The same calculations run on compressive films lead to pore volume fractions as low as 2.6% in average (contrary to ~17% in average for tensile films). For several of these films, this calculated fraction is even next to nil. This very small pore volume fraction suggests that free volumes are negligible in compressive films, i.e., nanopores and/or free volumes surrounding hydrogen atoms are virtually absent. The large mass density of these hydrogen-doped SiN compressive films (2.47–2.84 g/cm^3) is consistent with this comment.[31,34]

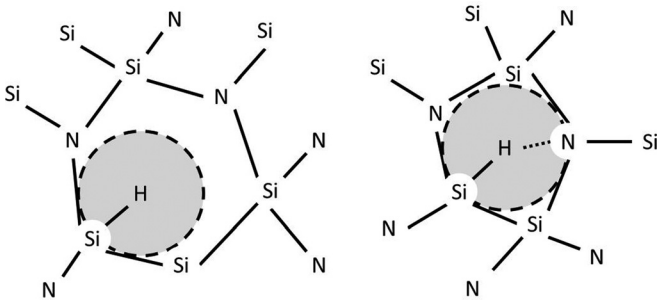

FIG. 9. Schematics of the behaviours of hydrogen in tensile (left) and compressive (right) films. In compressive films, hydrogen atoms sense neighbouring atoms because of the smaller available free volumes.

VI. DISCUSSION

At this point, some of the key results have to be reminded and merged for analysis. First, a discontinuous behaviour has been observed in stiffness evolution against negative volume fraction at the transition between tensile and compressive stresses (Figure 3). In tensile films, hydrogen atoms are shown to coexist with porosity (Figure 5) and to display a behaviour consistent with a pore-like behaviour (Figure 4). This last point implies that hydrogen atoms in tensile films are unable to transmit mechanical load (what was predicted from their only one chemical bonding). Conversely, hydrogen atoms behave differently in compressive films: free volumes are almost absent there (Figure 5) and the hydrogen impact on film density is no more consistent with a pore-like behaviour (Figure 4). This point has to be correlated with Figure 6 that explains the much smaller hydrogen radius observed in compressive films by the bond type (N-H bonds induce much less steric constraints that Si-H bonds do).

All these observations can be closely related to the mechanisms taking place when films are fabricated. During the processing of tensile films, the available free volumes are large enough to allow hydrogen to build-up large bonds (Figure 6), finally leading to mechanically relaxed single-bonded hydrogen atoms. However, during the processing of compressive films, the bonding of hydrogen atoms is highly constrained by the surrounding atom organisation (combined to atomic peening mechanism). As a consequence, the free volumes are too small to allow any kind of hydrogen bonding: the short interatomic distances are favoured (Figure 6), but even under this condition, the electron cloud of a bonded hydrogen senses neighbouring atoms, leading to an extra contribution of hydrogen to the global film stiffness (Figure 4). These two opposite mechanical behaviours in compressive and tensile films are schemed in Figure 9. An efficient way to merge these two behaviours will be presented elsewhere.[36]

As already stated, to our knowledge, no article has reported such a dual behaviour of hydrogen in SiN. This can be partially explained by the difficulty to process SiN films displaying such a large range of mechanical stresses (from −2.8 to 1.5 GPa in the present work) without either buckling or delaminating.[37] Moreover, literature preferentially relates hydrogen content to mechanical stress rather than to mechanical stiffness. For instance, Claassen *et al.*[20] and Paduschek *et al.*[38] both report that hydrogen desorption during thermal anneals is concomitant to a stress evolution from compressive to tensile state. Similar issues have been addressed on amorphous iono-covalent ceramics like amorphous-carbon, amorphous-silicon or amorphous-germanium. For instance, the pore-like behaviour of hydrogen has been observed in these systems under nil or tensile stress:[39–41] Kumagai *et al.* relate the softening of amorphous carbon with hydrogen incorporation to the free internal displacement of atoms allowed by these stress-free systems. Miranda *et al.* also report that hydrogen presence does not appear to influence the stiffness of fully relaxed amorphous silicon. This is in agreement with the pore-like behavior of hydrogen in our tensile films. Reported data on compressive films[41–44] have to be analyzed with care because no data are available on the porosity volume fraction which is, however, supposed to explain part of their results.[41] Nonetheless in all these works, hydrogen atoms affect directly the mechanical stress which means that they transmit mechanical load, i.e., they participate to the film stiffness, in accordance with our results. For instance, for low hydrogen content (<10%), Spanakis *et al.* report an almost linear Young's modulus increase with hydrogen increase.

VII. CONCLUSION

The present study on the mechanical influence of hydrogen and porosity on the mechanical stiffness of SiN films has emphasized the possibility to discriminate both volume fractions. The stiffer answer of compressive films than tensile films for similar f_{H+Pore} (negative phase volume fraction) is explained by a different mechanical behaviour of hydrogen in these two environments: hydrogen atoms behave mechanically like pores in tensile films (i.e., like zero-stiffness features), while they participate to film stiffness in compressive films because of steric effects. This conclusion has been drawn, thanks to (i) the introduction of a hydrogen-correction on the porosity volume fraction and to (ii) the calculation of the effective hydrogen radius (R_H).

[1]*Ceramic Interconnect Technology Handbook*, edited by F. D. Barlow III and A. Elshabini (CRC Press, 2010).
[2]*Handbook of Advanced Ceramics*, edited by S. Sōmiya *et al.* (Elsevier, 2003).
[3]*Handbook of Semiconductor Manufacturing Technology*, 2nd ed., edited by R. Doering and Y. Nishi (CRC Press, 2012).
[4]*Dielectric Films for Advanced Microelectronics*, edited by M. Baklanov, K. Maex, and M. Green (John Wiley & Sons, 2007).

[5]*Copper Interconnect Technology*, 2nd ed., edited by T. K. Gupta (Springer, 2009).
[6]E. Vanhove, A. Tsopéla, L. Bouscayrol, A. Desmoulin, J. Launay, and P. Temple-Boyer, Sens. Actuators, B **178**, 350–358 (2013).
[7]A. G. Aberle, Sol. Energy Mater. Sol. Cells **65**, 239 (2001).
[8]P. Morin, G. Raymond, D. Benoit, D. Guiheux, R. Pantel, F. Volpi, and M. Braccini, J. Vac. Sci. Technol., A **29**, 041513 (2011).
[9]J. F. Justo, F. de Brito Mota, and A. Fazzio, Phys. Rev. B **65**, 073202 (2002).
[10]P. Kroll, J. Non-Cryst Solids **293–295**, 238–243 (2001).
[11]F. de Brito Mota, J. F. Justo, and A. Fazzio, J. Appl. Phys. **86**, 1843 (1999).
[12]K. Jarolimek, R. A. de Groot, G. A. de Wijs, and M. Zeman, Phys. Rev. B **82**, 205201 (2010).
[13]H. Dun, P. Pan, F. R. White, and R. W. Douse, J. Electrochem. Soc. **128**, 1555 (1981).
[14]L. Smith, A. S. Alimonda, C.-C. Chen, S. E. Ready, and B. Wacker, J. Electrochem. Soc. **137**, 614 (1990).
[15]S. Hasegawa, Y. Amano, T. Inokuma, and Y. Kurata, J. Appl. Phys. **75**, 1493 (1994).
[16]I. Sugimoto, S. Nakano, and H. Kuwano, Thin Solid Films **268**, 152–160 (1995).
[17]W.-T. Li, D. R. McKenzie, W. D. McFall, and Q.-C. Zhang, Thin Solid Films **384**, 46–52 (2001).
[18]M. Gupta, V. K. Rathi, R. Thangaraj, O. P. Agnihotri, and K. S. Chari, Thin Solid Films **204**(1), 77–106 (1991).
[19]S. King, R. Chu, G. Xu, and J. Huening, Thin Solid Films **518**, 4898–4907 (2010).
[20]W. A. P. Claassen, W. G. J. M. Valkenburg, W. M. v. d. Wijgert, and M. F. C. Willemsen, Thin Solid Films **129**, 239–247 (1985).
[21]F. L. Martinez, R. Ruiz-Merino, A. del Prado, E. San Andres, I. Martil, G. Gonzalez-Diaz, C. Jeynes, N. P. Barradas, L. Wang, and H. S. Reehal, Thin Solid Films **459**, 203–207 (2004).
[22]D. Benoit, P. Morin, and J. Regolini, Thin Solid Films **519**, 6550–6553 (2011).
[23]H. T. Grahn, H. J. Maris, and J. Tauc, IEEE J. Quantum Electron. **25**, 2562 (1989).
[24]A. Devos and R. Cote, Phys. Rev. B **70**(12), 125208 (2004).
[25]A. Devos, R. Cote, G. Caruyer, and A. Lefebvre, Appl. Phys. Lett. **86**, 211903 (2005).
[26]M. Braccini, F. Volpi, A. Devos, G. Raymond, D. Benoit, and P. Morin, Thin Solid Films **551**, 120–126 (2014).
[27]A. Bondi, J. Phys. Chem. **68**(3), 441–451 (1964).
[28]A. M. Ukpong, M. Härting, and D. T. Britton, Philos. Mag. Lett. **88**(4), 293–302 (2008).
[29]L. J. Gibson and M. F. Ashby, *Cellular Solids: Structure and Properties* (Cambridge University Press, 1999).
[30]C. M. Flannery, C. Murray, I. Streiter, and S. E. Schulz, Thin Solid Films **388**, 1–4 (2001).
[31]B. A. Walmsley, Y. Liu, X. Z. Hu, M. B. Bush, K. J. Winchester, M. Martyniuk, J. M. Dell, and L. Faraone, J. Appl. Phys. **98**, 044904 (2005).
[32]K. K. Phani and S. K. Niyogi, J. Mater. Sci. Lett. **6**, 511–515 (1987).
[33]Z. Lu, Q. Liu, H. Han, and D. Zhang, Mater. Sci. Eng., A **559**, 201–209 (2013).
[34]H. Huang, K. J. Winchester, A. Suvorova, B. R. Lawn, Y. Liu, X. Z. Hu, J. M. Dell, and L. Faraone, Mater. Sci. Eng., A **435–436**, 453–459 (2006).
[35]H. He and M. F. Thorpe, Phys. Rev. Lett. **54**, 2107 (1985).
[36]F. Volpi, M. Braccini, A. Devos, G. Raymond, A. Pasturel, and P. Morin, "Merging the mechanical behaviours of compressive and tensile H-doped SiN films," Appl. Phys. Lett. (to be published).
[37]E. Johlin, N. Tabet, S. Castro-Galnares, A. Abdallah, M. I. Bertoni, T. Asafa, J. C. Grossman, S. Said, and T. Buonassisi, Phys. Rev. B **85**, 075202 (2012).
[38]P. Paduschek, C. Hopfl, and H. Mitlehner, Thin Solid Films **110**, 291–304 (1983).
[39]T. Kumagai, S. Sawai, J. Choi, S. Izumi, and T. Kato, J. Appl. Phys. **107**, 124315 (2010).
[40]C. R. Miranda, K. V. Tretiakov, and S. Scandolo, J. Non-Cryst. Solids **352**, 4283–4286 (2006).
[41]P. Tzanetakis, Sol. Energy Mater. Sol. Cells **78**, 369–389 (2003).
[42]D. Han, J. Baugh, and G. Yue, Phys. Rev. B **62**(11), 7169 (2000).
[43]E. Spanakis, E. Stratakis, P. Tzanetakis, and Q. Wang, J. Appl. Phys. **89**, 4294 (2001).
[44]M. M. de Lima, Jr. and F. C. Marques, Thin Solid Films **398–399**, 549–552 (2001).